Constr. Approx. (2004) 20: 549–564
DOI: 10.1007/s00365-003-0550-5

CONSTRUCTIVE APPROXIMATION

An Adaptive Mesh-Refining Algorithm Allowing for an H^1 Stable L^2 Projection onto Courant Finite Element Spaces

Carsten Carstensen

Abstract. Suppose $\mathcal{S}^1(\mathcal{T}) \subset H^1(\Omega)$ is the P_1-finite element space of $\mathcal{T}$-piecewise affine functions based on a regular triangulation $\mathcal{T}$ of a two-dimensional surface Ω into triangles. The L^2 projection Π onto $\mathcal{S}^1(\mathcal{T})$ is H^1 stable if $\|\Pi v\|_{H^1(\Omega)} \leq C\|v\|_{H^1(\Omega)}$ for all v in the Sobolev space $H^1(\Omega)$ and if the bound C does not depend on the mesh-size in $\mathcal{T}$ or on the dimension of $\mathcal{S}^1(\mathcal{T})$.

A red–green–blue refining adaptive algorithm is designed which refines a coarse mesh $\mathcal{T}_0$ successively such that each triangle is divided into one, two, three, or four subtriangles. This is the newest vertex bisection supplemented with possible red refinements based on a careful initialization. The resulting finite element space allows for an H^1 stable L^2 projection. The stability bound C depends only on the coarse mesh $\mathcal{T}_0$ through the number of unknowns, the shapes of the triangles in $\mathcal{T}_0$, and possible Dirichlet boundary conditions. Our arguments also provide a discrete version $\|h_{\mathcal{T}}^{-1}\,\Pi v\|_{L^2(\Omega)} \leq C\|h_{\mathcal{T}}^{-1}\,v\|_{L^2(\Omega)}$ in L^2 norms weighted with the mesh-size $h_{\mathcal{T}}$.

1. Introduction

This paper concerns triangulations of a two-dimensional compact polyhedral manifold Ω into triangles, i.e., $\mathcal{T}$ is a set of closed triangles T in $\overline{\Omega} \subset \mathbf{R}^n$ with

$$\bigcup \mathcal{T} = \overline{\Omega} \subset\subset \mathbf{R}^n.$$

The triangulations are regular in the sense of Ciarlet, i.e., each nonvoid intersection of two distinct triangles is either a joint vertex or a common edge of both triangles.

Each triangulation $\mathcal{T}$ induces a finite element space $\mathcal{S}^1(\mathcal{T})$, the $\mathcal{T}$-piecewise affine and globally continuous functions,

$$\mathcal{S}^1(\mathcal{T}) := \{v \in C^0(\Omega) : \forall\, T \in \mathcal{T},\ v|_T \text{ affine}\}.$$

Given a coarse regular triangulation $\mathcal{T}_0$, an adaptive algorithm generates a sequence of triangulations by red–green–blue refinement which divides each triangle into one, two,

Date received: May 15, 2002. Date revised: January 2, 2003. Date accepted: May 1, 2003. Communicated by Peter Oswald. Online publication: October 10, 2003.
AMS classification: 65N30, 65R20, 73C50.
Key words and phrases: Finite element method, L^2 Projection, H^1 Stability, Adaptive algorithm, Newest-vertex bisection.

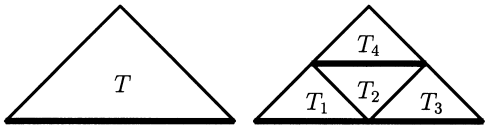

Fig. 1. Red refinement of a triangle T into $T_1, \ldots, T_4$; thick edges indicate old and new reference edges.

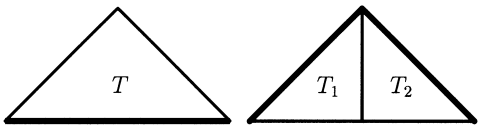

Fig. 2. Green refinement of a triangle T into T_1 and T_2; thick edges indicate old and new reference edges.

three, or four subtriangles as illustrated in Figures 1, 2, and 3. The concept and refinement of a reference edge, made precise in Section 2, essentially avoid degeneracies, e.g., maintain the minimum angle condition. In this paper, it also avoids overrefinements.

In the literature we find a priori [9], [6] and a posteriori [3], [13] conditions on the decay of the mesh-size in terms of a distance of two elements which are sufficient for the H^1 stability of Π. The observation [6] that the red–green–blue refinement strategy controls overrefinements motivated this paper. We design Algorithms 2.1 and 2.2 which steer the selection of reference edges in the coarse triangulation $\mathcal{T}_0$ and in any red–green–blue refinement step. The main purpose of Algorithms 2.1 and 2.2 is that any induced finite element space allows for a stable L^2 projection. The two algorithms do not bisect the longest edge (see, e.g., [12] for details on this alternative); instead we follow the newest-vertex bisection supplemented with possible red refinement steps (see Figures 1, 2, and 3).

Let $\mathcal{E}_0$ (resp., $\mathcal{E}$) denote the edges in $\mathcal{T}_0$ (resp., $\mathcal{T}$) and let $\mathcal{E}_D \subseteq \mathcal{E}_0$ denote the (possibly empty) set of edges on the (possibly empty) Dirichlet boundary $\Gamma_D = \bigcup \mathcal{E}_D$. Set

$$
\begin{aligned}
H^1_D(\Omega) &:= \{v \in C^0(\Omega) : \forall\, T \in \mathcal{T}_0,\, v|_T \in H^1(T) \text{ and } v|_{\Gamma_D} = 0\},\\
\mathcal{S}^1_D(\mathcal{T}) &:= \{v \in H^1_D(\Omega) : \forall\, T \in \mathcal{T},\, v|_T \text{ affine}\}.
\end{aligned}
$$

Let ∇ denote the $\mathcal{T}_0$-piecewise two-dimensional gradient. Then, the formula

$$
\|\nabla v\|^2_{L^2(\Omega)} + \|v\|^2_{L^2(\Omega)} = \|v\|^2_{H^1(\Omega)}
$$

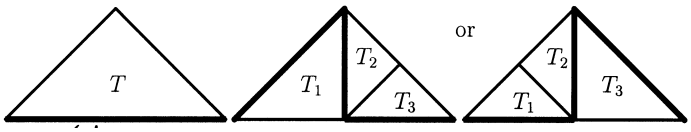

Fig. 3. The two possible blue refinements of a triangle T into T_1, T_2, T_3; thick edges indicate old and new reference edges. Each blue refinement consists of two consecutive green refinement steps.

defines the norm in the Sobolev space $H^1(\Omega)$. Our main result asserts the H^1 stability of the L^2 projection

$$\Pi : L^2(\Omega) \to L^2(\Omega)$$

onto the finite element space $\mathcal{S}^1_D(\mathcal{T})$.

Theorem 1. *Let $\mathcal{T}_0$ be a regular triangulation of the bounded two-dimensional piecewise planar Lipschitz manifold $\Omega \subseteq \mathbf{R}^n$. Let $\mathcal{T}$ be a red–green–blue refinement of $\mathcal{T}_0$ generated by Algorithm* 2.1 *and L steps of Algorithm* 2.2. *Then, for any $v \in H^1_D(\Omega)$, we have $\Pi v \in \mathcal{S}^1_D(\Omega)$ with*

$$\|\nabla \Pi v\|_{L^2(\Omega)} \leq \|\Pi\| \, \|\nabla v\|_{L^2(\Omega)} \quad \textit{and} \quad \|h_{\mathcal{T}}^{-1} \, \Pi v\|_{L^2(\Omega)} \leq \|\Pi\| \, \|h_{\mathcal{T}}^{-1} v\|_{L^2(\Omega)}.$$

The bound $\|\Pi\|$ for the L^2 projection Π onto $\mathcal{S}^1_D(\mathcal{T})$ depends on $\mathcal{T}_0$ and Γ_D but is independent of L or $\operatorname{card}(\mathcal{T})$.

The remaining part of the paper is organized as follows. Section 2 introduces the concepts of regular triangulations, red–green–blue refinements, reference edges, and the two algorithms of Theorem 1. The key result of Proposition 3.1 in Section 3 bounds the decay of refinement levels of three connected elements in the class of triangulations under consideration. This is the basis of Proposition 4.1 in Section 4 which then defines a quantity d_z for each node $z \in \mathcal{N}$. Neighboring nodes a and b satisfy $d_a/d_b \leq \sqrt{8}$ and d_z is equivalent to mesh-sizes of elements with vertex z. These properties permit a proof of Theorem 1 in Section 5 with the theory of [6] based on [13], [3].

2. Adaptively Refined Triangulations

The piecewise planar Lipschitz surface Ω is a connected and closed two-dimensional manifold decomposed by a coarse triangulation $\mathcal{T}_0$: Each $T \in \mathcal{T}_0$ is a closed triangle in $\mathbf{R}^n$, i.e., the convex hull of the three vertices, called nodes, and has a positive two-dimensional measure $|T|$.

Definition 2.1. A triangulation $\mathcal{T}$ of Ω is *regular* if two distinct triangles T_1 and T_2 in $\mathcal{T}$ are either disjoint, $T_1 \cap T_2 = \emptyset$, or share exactly one node $z \in \mathbf{R}^n$, $T_1 \cap T_2 = \{z\}$, or share exactly one edge $E = \operatorname{conv}\{a, b\}$, $T_1 \cap T_2 = E$, that combines two vertices a, b of both, T_1 and T_2.

In particular, each vertex of some triangle in a regular triangulation intersects with other triangles at precisely one of their vertices (hanging nodes are not allowed, see, e.g., [4], [7]).

Definition 2.2. Given a regular triangulation $\mathcal{T}$, let $\mathcal{N}$ denote the nodes in $\mathcal{T}$ (i.e., the set of all possible vertices of triangles in $\mathcal{T}$) and let $\mathcal{E}$ denote the edges (i.e., the set of all possible edges E of triangles in $\mathcal{T}$).

A fundamental concept within the green and blue refinements is the reference edge of an element [2], [11], [10], [1].

Definition 2.3. For each element K in the coarse triangulation $\mathcal{T}_0$, let $E(K) \in \mathcal{E}_0$ denote one of the three edges, called the reference edge of K. An element $T \in \mathcal{T}_0$ is called *isolated* if the reference edge $E(T)$ is shared with another element $K \in \mathcal{T}_0$, $E(T) = T \cap K$, with a different reference edge $E(K) \neq E(T)$.

Remark 2.1. In the literature on element bisection, a *reference edge* is often called *marked edge*. In this paper, however, we introduced the word *reference* to distinguish between marked objects (elements or edges) which will currently be refined in the mesh-generation step at hand and those which mark an object to steer the refinement rules which may or may not be executed within the design of forthcoming meshes.

The following algorithm generates the reference edges of a given coarse triangulation in a proper way, i.e., two distinct isolated elements do not share an edge.

Algorithm 2.1. (Define Reference Edges for the Coarse Triangulation) *Input is a coarse triangulation* $\mathcal{T}_0$. Set $\mathcal{T}^{(0)} := \mathcal{T}_0$ and $j := 0$.

```
Repeat
      Choose T∈T^(j) and look for K∈T^(j) with T∩K=E∈E_0.
      If such K∈T^(j) exist,
           choose one of them and set E(T) := T∩K =: E(K).
           Set T^(j+1) := T^(j)\{T, K} and j := j+1.
           (Note that neither T nor K is isolated.)
      If no such K exists,
           choose some edge E of T and set E(T) := E,
           T^(j+1) := T^(j)\{T}, and j := j+1.
Until T^(j) = ∅.
```

Output is $E(T)$ *for all* $T \in \mathcal{T}_0$.

Proposition 2.1.

(a) *Algorithm* 2.1 *is feasible in the sense that it defines one reference edge* $E(T)$ *for each triangle* T *in* $\mathcal{T}_0$ *in at most* $\operatorname{card}(\mathcal{T}_0)$ *steps*.
(b) *Two distinct isolated elements in* $\mathcal{T}_0$ *cannot share an edge*.

Proof. Part (a) follows from the fact that $\mathcal{T}^{(j+1)}$ equals $\mathcal{T}^{(j)}$ reduced by one or two elements and so stops after at most $\operatorname{card}(\mathcal{T}_0)$ steps. Suppose that (b) is wrong, i.e., assume K and T share an edge and that their (distinct) reference edges are defined in steps k and ℓ of Algorithm 2.1. We have $k \neq \ell$ as K and T are distinct and isolated. Also $k < \ell$ is impossible as then $T, K \in \mathcal{T}^{(k)} = \mathcal{T}^{(k+1)} \cup \{K\}$ but $T \cap K \in \mathcal{E}_0$ and so this situation cannot arise. The same arguments prohibit $\ell < k$ as well. This concludes the proof. ■

The red–green–blue refinements divide a triangle T with reference edge $E(T)$ into one, two, three, or four subtriangles and define their reference edges. Besides no refinement (i.e., $T \mapsto T$) there are the three rules of Figures 1, 2, and 3.

Example 2.1 (Red). A triangle T is decomposed into four congruent scaled copies T_1, T_2, T_3, T_4 of it such that the edges' midpoints are the new nodes. The mapping $T \mapsto (T_1, T_2, T_3, T_4)$ is called red refinement. The old and new reference edges are depicted in Figure 1.

Example 2.2 (Green). A triangle T is halved along its reference edge $E(T)$. The green refinement $T \mapsto (T_1, T_2)$ is depicted in Figure 2 with the old and new reference edges.

Example 2.3 (Blue). Two successive green refinements of a triangle T describe one blue refinement $T \mapsto (T_1, T_2, T_3)$ depicted with reference edge in Figure 3. Notice that either of the two nonreference edges of T could be refined and hence the two resulting variants are shown.

In each step of our adaptive mesh-refining algorithm, we are given a set of edges $\mathcal{E}_{(j)}$ which will be refined.

Algorithm 2.2 (Adaptive Mesh-Refining). *Input is the coarse triangulation $\mathcal{T}_0$ with reference edges $E(T)$, $T \in \mathcal{T}_0$, from Algorithm* 2.1.
Set $\mathcal{T}^{(0)} := \mathcal{T}_{(0)}$ and $j := 0$.
Repeat
  Select a set of edges $\mathcal{E}_{(j)}$ such that each triangle $T \in \mathcal{T}_{(j)}$ with edge $E \in \mathcal{E}_{(j)}$ satisfies $E(T) \in \mathcal{E}_{(j)}$.
  Perform red-green-blue or no refinement of $T \in \mathcal{T}_{(j)}$ with edges E_1, E_2, E_3 such that $\{E_1, E_2, E_3\} \cap \mathcal{E}_{(j)}$ are halved.
  Set new triangulation $\mathcal{T}_{(j+1)}$ with new set of reference edges $(E(T) : T \in \mathcal{T}_{(j+1)})$ and $j := j + 1$.
Until $\mathcal{E}_{(j)} = \emptyset$.
Output is triangulation $\mathcal{T} = \mathcal{T}_{(j)}$.

Example 2.4. In each step of Algorithm 2.2 we are given a set $\mathcal{E}_{(j)}$ of edges which will be refined. This set is frequently defined by element-oriented refinement indicators [14]. For instance, if $\mathcal{M}_{(j)}$ is a set of marked elements in $\mathcal{T}_{(j)}$, we may set

$$\begin{aligned} \mathcal{E}_{(j)}^{(0)} &:= \{E \text{ edge of } T : T \in \mathcal{M}_{(j)}\} \quad \text{and, for } k = 0, 1, 2, \ldots, \\ \mathcal{E}_{(j)}^{(k+1)} &:= \{E(T) : \exists\, T \in \mathcal{T}_{(j)} \text{ with edge in } \mathcal{E}_{(j)}^{(k)}\} \cup \mathcal{E}_{(j)}^{(k)}. \end{aligned}$$

The increasing sequence $\mathcal{E}_{(j)}^{(0)} \subseteq \mathcal{E}_{(j)}^{(1)} \subseteq \ldots \subseteq \mathcal{E}_{(j)}$ will become constant $\mathcal{E}_{(j)} = \mathcal{E}_{(j)}^{(k)}$ for sufficiently large k. Then, Algorithm 2.2 red refines each T in $\mathcal{M}_{(j)}$ and red–green–blue refines further elements. It satisfies the condition that each $T \in \mathcal{M}_{(j)}$ with edge $E \in \mathcal{E}_{(j)}$ satisfies $E(T) \in \mathcal{E}_{(j)}$ and so avoids hanging nodes.

The output of Algorithm 2.2 has some particular properties.

Proposition 2.2.

(a) *Algorithm* 2.2 *generates a regular triangulation* $\mathcal{T}$ *which is a refinement of* $\mathcal{T}_0$.
(b) *For each* $T \in \mathcal{T}$ *there exists exactly one* $K \in \mathcal{T}_0$ *with* $T \subseteq K$.
(c) *Each* $K \in \mathcal{T}_0$ *with reference edge* $E(K)$ *uniquely defines an affine map* $\Phi : K \to T_{\mathtt{ref}}$ *onto the reference triangle* $T_{\mathtt{ref}} = \mathrm{conv}\{(0,0), (0,1), (1,0)\}$ *by* $\Phi(E(K)) = \mathrm{conv}\{(0,1), (1,0)\}$ *and* $\det D\Phi > 0$. *The triangulation*

$$\hat{T}_K := \{\Phi(T) : \ T \in \mathcal{T}, T \subseteq K\} \text{ of } K$$

consists of right isosceles triangles. (*A right isosceles triangle results from a square halved along a diagonal*.)

Proof. By mathematical induction on j in Algorithm 2.2. In (c) we use that any red–green–blue refinement of a right isosceles triangle results into right isosceles triangles. ∎

Remark 2.2. Some bisection algorithms in the literature are based on successive refinements in order to guarantee that at least the reference edge of each refined element is bisected. This is occasionally called closure algorithm. Algorithm 2.2 assumes this implicitly in the first two lines of the repeat loop through a selection of $\mathcal{E}_{(j)}$ such that each triangle $T \in \mathcal{T}_{(j)}$ with edge $E \in \mathcal{E}_{(j)}$ satisfies $E(T) \in \mathcal{E}_{(j)}$. Given any set $\mathcal{E}_{(j,0)}$ of marked edges in the current triangulation (e.g. selected by refinement indicators), $\mathcal{E}_{(j,0)}$ is successively enlarged eventually to obtain $\mathcal{E}_{(j)}$ with the required property. This functions as a closure algorithm to guarantee a regular triangulation.

Remark 2.3. The selection of a reference edge by Algorithm 2.1 seems to be new. The condition in this paper that isolated elements are not neighbors (via a shared edge) is less restrictive than that of no isolated triangles at all (in the triangulation). The later condition is that all triangles are compatibly divisible and employed to maintain regularity [11, Algorithm 2.1].

We conclude Section 2 on adapted meshes with a comparison to another red–green–blue refinement algorithm which differs by another choice of the reference edges, namely by the longest edge strategy.

Example 2.5. Figure 4 shows six configurations to illustrate the difference of two possible refinement algorithms. The left column depicts three triangulations of the triangle (A, B, C) while the right column displays the affine image of the left; A, B, C is mapped onto A', B', C', etc. Let us start with the first row. The triangle A, B, C is special in that the length $|AB|$ of the edge $\overline{AB} := \mathrm{conv}\{A, B\}$ is smaller than $|AC| = |BC|$. Suppose $\overline{AC} = E(A, B, C)$ is the reference edge in all algorithms. The affine image reflects this in that $\overline{A'C'}$ is the diagonal of the reference triangle. Any red refinement of (A, B, C) would yield four congruent smaller configurations which essentially coincide with (A, B, C), so let us look at one green refinement. The reference edge $\overline{AC}$ is divided at D and we obtain the first picture in Figure 4. The triangle (A, B, C) is special in that

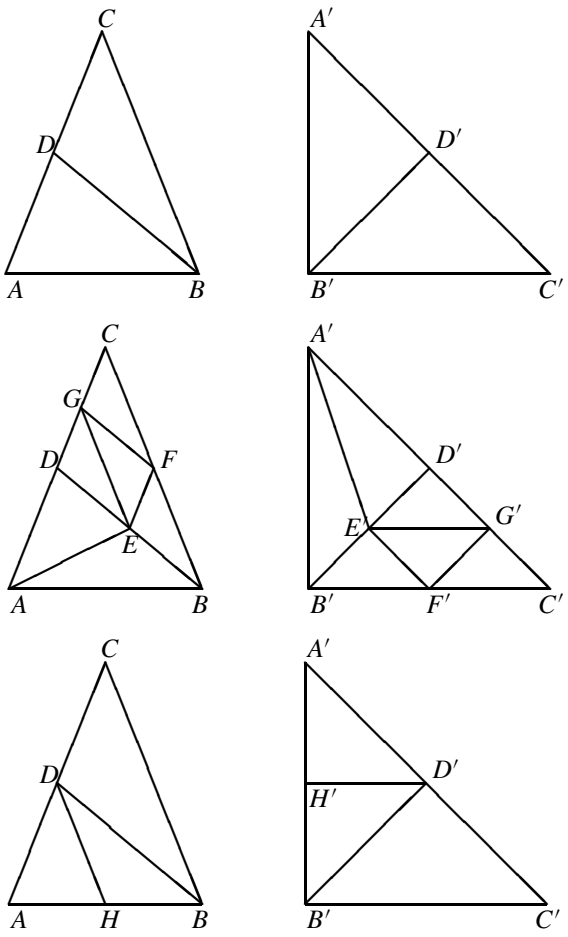

Fig. 4. One green refinement of a triangle (A, B, C) (top) followed by one of (A, B, D) with respect to reference edge $\overline{BD}$ (middle) or $\overline{AB}$ (bottom). The right column displays the affine image onto the reference triangle (A', B', C'). Algorithm 2.2 avoids the middle configuration by $E(A, B, D) = \overline{AB}$.

$|AB| = |DB|$. Hence the longest edge strategy may choose either the reference edge $\overline{BD}$ or the reference edge $\overline{AB}$, while our strategy insists on $\overline{AB}$. A different scaling of the vertical axis changes the reference choice: If we enlarge the distance of C onto $\overline{AB}$, $|AB| < |BD|$ and the longest edge strategy uniquely chooses the reference edge $|BD|$. A green (resp., red) refinement in the two triangles of the top figures results in the situation of the middle pictures. We see clearly that $\overline{A'E'}$ does not yield right isosceles triangles in the affine image on the right. If, conversely, the distance of C to $\overline{AB}$ is smaller than in Figure 4, $|BD| < |AB|$ and in both reference choices we have $E(A, B, D) = \overline{AB}$. A green refinement in (A, B, D) leads to the bottom pictures of Figure 4. The point is that the affine image consists of right isosceles triangles.

Remark 2.4. The example clearly illustrates, first, our red–green–blue refining algorithm is different to the usually proposed longest-edge strategy; second, the latter algorithm does, in general, not lead to affine images of triangulations into right isosceles triangles, whereas Algorithm 2.2 does; third, the number of different angles in the triangulation generated for the longest-edge strategy is, in general, larger than (or at least equal to) in Algorithm 2.2.

3. Mesh-Size Decay in Adapted Triangulations

Throughout this section, we consider a regular triangulation $\mathcal{T}$ of Ω obtained by Algorithms 2.1 and 2.2.

Definition 3.1 (Distance of Nodes). Given two distinct nodes a and b in $\mathcal{N}$ let $\delta(a, b)$ be the smallest integer J such that J elements $T_1, T_2, \ldots, T_J \in \mathcal{T}$ exist with $a \in T_1$, $T_1 \cap T_2 \neq \emptyset$, $T_2 \cap T_3 \neq \emptyset$, $\ldots$, $T_{J-1} \cap T_J \neq \emptyset$ and $b \in T_J$; set $\delta(z, z) = 0$ for each $z \in \mathcal{N}$.

Remark 3.1. $(\mathcal{N}, \delta)$ is a metric space.

Definition 3.2 (Level of Refinement). For each $T \in \mathcal{T}$ we define $\ell(T) \geq 0$ through the macroelement $K \in \mathcal{T}_0$ with $T \subseteq K$ by

$$\ell(T) := \log_2 \sqrt{|K|/|T|}$$

where $|T|$ denotes the area of an element T.

Remark 3.2. By mathematical induction, we infer

$$\ell(T) \in \{0, \tfrac{1}{2}, 1, \tfrac{3}{2}, 2, \ldots\}.$$

The subsequent decay estimate is the key observation for the stability proof.

Proposition 3.1. *Suppose $a, b \in \mathcal{N}\backslash\mathcal{N}_0$, $\delta(a, b) \leq 1$, $a \in T$, $b \in K$ for $T, K \in \mathcal{T}$. Then,*

$$|\ell(T) - \ell(K)| \leq 3.$$

Proof. Before we immerse ourselves in the most complicated configurations possible in $\mathcal{T}$, we stress the setting and the difficulty of this proof. Proposition 2.2(c) guides us to consider right isosceles triangles which share one vertex z. There exists only a finite number of shapes of such patches $\omega_z = \bigcup\{T \in \mathcal{T} : z \in T\}$ and Figure 5 shows one of those. The assertion gives a useful estimate of different mesh-sizes (relative to macro elements) of two elements in two overlapping patches. The patch $\hat{\omega}_z$ of Figure 5 is extremal in the sense that $|T_6|/|T_1| = 8$ is the maximal quotient of the area for two elements of one patch. The proposition asserts that T and K allow such estimates for one element $M \in \mathcal{T}$ with $a, b \in M$, namely,

$$|K|/|M| \leq 8 \qquad \text{and} \qquad |M|/|T| \leq 8.$$

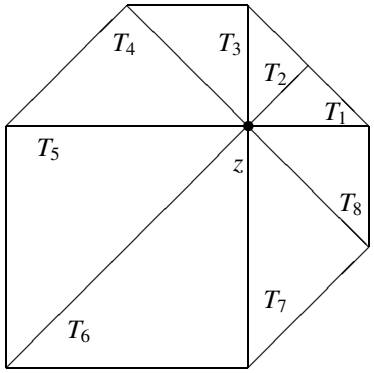

Fig. 5. Extremal patch $\tilde{\omega}_z$ within a triangulation into right isosceles triangles.

In the simplest configuration, all three elements T, M, K belong to the same macroelement K_0. Then

$$\begin{aligned}\ell(T) - \ell(K) &= \log_2 \sqrt{|K_0|/|T|} - \log_2 \sqrt{|K_0|/|K|} \\ &= \tfrac{1}{2} \log_2(|K|/|T|) \leq \tfrac{1}{2} \log_2 64 = 3.\end{aligned}$$

This is the idea of the proposition. The difficulty is that all three elements may belong to different macroelements and with possibly quite different areas. Nevertheless, Algorithms 2.1 and 2.2 provide sufficient structural uniformity to maintain the above estimate in any possible situation.

After the introduction to the simplest configuration, we consider the most complicated configuration. For simpler situations several steps below are redundant. It can indeed happen that $T \subseteq T_0$ and $K \subseteq K_0$ belong to two distinct macroelements T_0 and K_0 in $\mathcal{T}_0$ and that edge $E \in \mathcal{E}$ between a and b does neither belong to T_0 nor to K_0. Since neither a nor b are nodes in the coarse triangulation $\mathcal{T}_0$, then a and b belong to the boundary of another macroelement $M_0 \in \mathcal{T}_0$ with $a \in M_0 \cap T_0 \in \mathcal{E}_0$ and $b \in M_0 \cap K_0 \in \mathcal{E}_0$. Let us map M_0 to the reference element as in Proposition 2.2. For the node a (resp., b) we proceed as follows. If a (resp., b) belongs to the reference edge of both M_0 and T_0 (resp., M_0 and K_0) or if it belongs to neither of the two, we map T_0 (resp., K_0) to the reference element and translate and rotate the image such that it fits the corresponding edge of $T_{\mathtt{ref}}$ to which a (resp., b) is mapped by the first mapping. In case that a (resp., b) belongs to the reference edge of M_0 but not to that of T_0 (resp., K_0) we scale the picture of the map onto $T_{\mathtt{ref}}$ by a factor $\sqrt{2}$ and then translate and rotate to fit the two images of the edge $M_0 \cap T_0$ (resp., $K_0 \cap T_0$). In the remaining case, a (resp., b) does belong to the reference edge of T_0 (resp., K_0) but does not belong to the reference edge of M_0. Then we scale the affine image of T_0 (resp., K_0) by a factor $1/\sqrt{2}$ and rotate and translate it to fit the two images of the edge $M_0 \cap T_0$ (resp., $K_0 \cap T_0$). The resulting macroelement configuration is of the form shown in Figure 6 (we neglected some variants which are symmetric to one of the displayed forms).

Because of Proposition 2.1(b), the configurations of Figure 7 cannot arise: In all cases shown, the reference edges of T_0 and M_0 as well as of M_0 and K_0 do not coincide and so two neighboring macroelements are isolated. In conclusion, at least two of the three

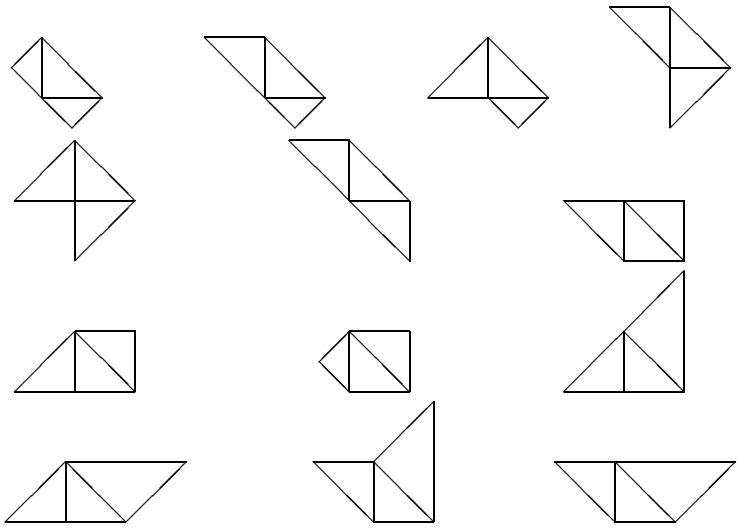

Fig. 6. Some possible $\mathcal{T}_0$-piecewise affine images $\tilde{K}_0$, $\tilde{M}_0, \tilde{T}_0$ of three neighboring macroelements K_0, M_0, T_0 in the proof of Proposition 3.1. Other variants are obtained by reflection along the main diagonal.

triangles shown in the configurations of Figure 6 are congruent. Let us denote the image of K_0, M_0, and T_0 under the $\mathcal{T}_0$-piecewise affine mapping, that are possibly among the configurations of Figure 6, by $\tilde{K}_0$, $\tilde{M}_0$, and $\tilde{T}_0$, respectively. Then

$$|\tilde{K}_0|/|\tilde{T}_0| \leq 2.$$

Owing to Proposition 2.2, the image of $\mathcal{T}|_{(M_0 \cup K_0 \cup T_0)}$ onto $\tilde{K}_0 \cup \tilde{M}_0 \cup \tilde{T}_0$ yields a triangulation $\tilde{\mathcal{T}}$ of $\tilde{K}_0 \cup \tilde{M}_0 \cup \tilde{T}_0$ into right isosceles triangles. Within the triangulation $\tilde{\mathcal{T}}$, the patch of the node $z := \tilde{a}$ (resp., $z := \tilde{b}$) consists of at most eight triangles (at most four if z belongs to an edge on the relative boundary $\partial\Omega$ of Ω). Figure 5 shows such an example.

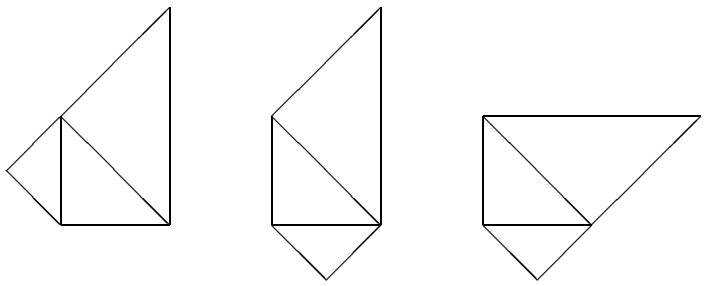

Fig. 7. Impossible $\mathcal{T}_0$-piecewise affine images $\tilde{K}_0$, $\tilde{M}_0$, $\tilde{T}_0$ of three neighboring macroelements K_0, M_0, T_0 in the proof of Proposition 3.1. The three configurations are avoided by Algorithm 2.1.

The patch $\tilde{\omega}_z$ of Figure 5 is extremal in the sense that for two triangles T and K in this patch we have

$$|K|/|T| \leq 8$$

and equality is possible, e.g., $|T_5|/|T_1| = 8$. However, for any other patch (i.e., different from a scaled and rotated version of $\tilde{\omega}_z$) we have

$$|K|/|T| \leq 4.$$

The images $\tilde{K}$ and $\tilde{T}$ of K and T belong to overlapping patches $\tilde{\omega}_a$ and $\tilde{\omega}_b$, $\delta(a, b) = 1$. With any element $\tilde{M}$ in their intersection, we deduce

$$|\tilde{K}|/|\tilde{M}| \leq 8 \qquad \text{and} \qquad |\tilde{M}|/|\tilde{T}| \leq 8.$$

Since two patches of the form of Figure 5 but of different size cannot be overlapping neighbors, we have that only one equality is possible and the other inequality can be replaced by ≤ 4. Thus,

$$|\tilde{K}|/|\tilde{T}| = |\tilde{K}|/|\tilde{M}| \ \ |\tilde{M}|/|\tilde{T}| \leq 8 \cdot 4 = 32.$$

Recall the above estimate $|\tilde{T}_0|/|\tilde{K}_0| \leq 2$ to conclude

$$|\tilde{T}_0|/|\tilde{T}| \ |\tilde{K}|/|\tilde{K}_0| \leq 64.$$

Moreover, $\tilde{T}_0$ and $\tilde{T}$ (resp., $\tilde{K}_0$ and $\tilde{K}$) are images of the same affine map and so their quotient of areas is preserved,

$$|\tilde{T}_0|/|\tilde{T}| = |T_0|/|T| \qquad (\text{resp., } |\tilde{K}|/|\tilde{K}_0| = |K|/|K_0|).$$

Therefore, we have

$$\begin{aligned} \ell(T) - \ell(K) &= \log_2 \sqrt{|T_0|/|T| \ |K|/|K_0|} \\ &= \log_2 \sqrt{|\tilde{T}_0|/|\tilde{T}| \ |\tilde{K}|/|\tilde{K}_0|} \\ &\leq \log_2 \sqrt{64} = 3. \end{aligned}$$

This concludes the proof (as K and T play symmetric roles in Proposition 3.1 and so can be interchanged). ■

4. Two Basic Estimates

With the decay estimate of Proposition 3.1 we can define an auxiliary nodal value d_z introduced in [6].

Definition 4.1. For each node $z \in \mathcal{N}$ we define

$$d_z := \min_{T \in \mathcal{T}} 2^{3/2\,\delta(z,T) - \ell(T)}, \quad \text{where} \quad \delta(z, T) := \min\{\delta(z, x) : x \in \mathcal{N} \cap T\}.$$

Proposition 4.1.

(a) *For $a, b \in \mathcal{N}$ with $\delta(a,b) = 1$ we have*

$$d_a/d_b \leq \sqrt{8}.$$

(b) *There exists a constant $c_1 = c_1(\mathcal{T}_0)$ which depends on $\mathcal{T}_0$ (but not on $\mathcal{T}$ or* $\mathrm{card}(\mathcal{T})$ *or mesh-sizes) such that, for all $z \in \mathcal{N}$ and $T \in \mathcal{T}$ with $z \in T$, we have*

$$d_z^2/|T| + |T|/d_z^2 \leq c_1.$$

Proof. For $b \in \mathcal{N}$ let $T \in \mathcal{T}$ satisfy $d_b = 2^{3/2\,\delta(b,T)-\ell(T)}$. Given $a \in \mathcal{N}$ with $\delta(a,b) = 1$, we have $\delta(a,T) \leq 1 + \delta(b,T)$. Then,

$$d_a \leq 2^{3/2\,\delta(a,T)-\ell(T)} \qquad \text{and so} \qquad d_a/d_b \leq 2^{3/2(\delta(a,T)-\delta(b,T))} \leq \sqrt{8}.$$

This proves (a). Since $\delta(z,T) = 0$ in (b) we infer

$$d_z^2/|T| \leq (2^{3/2\,\delta(z,T)-\ell(T)})^2/|T| = 2^{-2\ell(T)}/|T|.$$

By definition of $\ell(T)$ for $T \subseteq \hat{T} \in \mathcal{T}_0$, we have

$$d_z^2/|T| \leq 2^{-\log_2(|\hat{T}|/|T|)}/|T| = 1/|\hat{T}|$$

which depends on $\mathcal{T}_0$ only. This shows the first estimate in (b). The remaining proof of the second estimate requires Proposition 3.1. Let

$$d_z = 2^{3/2\,\delta(z,K)-\ell(K)}$$

for a minimizing $K \in \mathcal{T}$. Let $J = \delta(z,K) + 1$ be the minimal number of elements $T_1, T_2, \ldots, T_J$ such that $z \in T_1$, $T_1 \cap T_2 \neq \emptyset$, $T_2 \cap T_3 \neq \emptyset$, …, $T_{J-1} \cap T_J \neq \emptyset$, and $T_J = K$. There are only a finite number of nodes in the coarse triangulation, $\mathrm{card}(\mathcal{N}_0)$, and so, for a bounded number of intersections $T_j \cap T_{j+1}$, we have

$$T_j \cap T_{j+1} \cap \mathcal{N} \subseteq \mathcal{N}_0.$$

Note carefully, that an infinite loop is not allowed, as the intersections $T_1 \cap T_2$, $T_2 \cap T_3$, …, $T_{J-1} \cap T_J$ are pairwise disjoint (otherwise, we could link z and K with a smaller number of elements). Hence we have $L \leq \mathrm{card}(\mathcal{N}_0)$ indices $j_1 < j_2 < \cdots < j_L < J$ with

$$T_{j_\ell+1} \cap T_{j_\ell+2},\ T_{j_\ell+2} \cap T_{j_\ell+3},\ \ldots,\ T_{j_{\ell+1}-1} \cap T_{j_{\ell+1}}$$

is different from $\{x\}$ for some $x \in \mathcal{N}_0$ or from E for some $E \in \mathcal{E}_0$, $\ell = 1, \ldots, L-1$. Only the L exceptions $T_{j_\ell} \cap T_{j_\ell+1}$, $\ell = 1, 2, \ldots, L$, may have this form. Given $\ell = 1, 2, \ldots, L$, we consider

$$T_m, T_{m+1}, \ldots, T_n \qquad \text{for} \quad m = j_\ell + 1 \text{ and } n = j_{\ell+1}.$$

The triples (T_m, T_{m+1}, T_{m+2}), $(T_{m+2}, T_{m+3}, T_{m+4})$, $(T_{m+4}, T_{m+5}, T_{m+6})$, …, $(T_{m+2\mu}, T_{m+2\mu+1}, T_{m+2\mu+2})$ for $m+2\mu+2 = n$ or $n-1$ satisfy the conditions of Proposition 3.1.

Indeed, for $T_{m+2\nu}, T_{m+2\nu+1}, T_{m+2\nu+2}$ we find $a, b \in \mathcal{N}\backslash\mathcal{N}_0$ with $a \in T_{m+2\nu} \cap T_{m+2\nu+1}$ and $b \in T_{m+2\nu+1} \cap T_{m+2\nu+2}$, whence $\delta(a, b) \leq 1$. Therefore,

$$|\ell(T_{m+2\nu}) - \ell(T_{m+2\nu+2})| \leq 3.$$

Triangle inequalities show

$$|\ell(T_m) - \ell(T_{m+2\mu+2})| \leq 3(\mu + 1).$$

Proposition 3.1 is applicable to (T_{n-1}, T_n, T_n) as well and we infer

$$|\ell(T_{m+2\mu+2}) - \ell(T_n)| \leq 3.$$

Altogether (in all cases, $n - m$ even or odd),

$$|\ell(T_m) - \ell(T_n)| \leq \tfrac{3}{2}(n - m + 1).$$

This reads, for $\ell = 1, 2, \ldots, L$,

$$|\ell(T_{j_\ell+1}) - \ell(T_{j_{\ell+1}})| \leq \tfrac{3}{2}(j_{\ell+1} - j_\ell).$$

For each $z \in \mathcal{N}_0$ with $z \in T_{j_\ell} \cap T_{j_\ell+1}$, there are a limited number of elements in the patch of z; one bound is $2\,\mathrm{card}(\mathcal{T}_0)$ (as $\mathcal{T}_0$ contains $\leq \mathrm{card}(\mathcal{T}_0)$ elements in the coarse mesh and this could be doubled at most by refinements).

The quotient of two areas of two neighboring elements is bounded by a constant which depends on the shape of the elements only. Hence, there is a constant $c_2 \geq 1$, that depends only on $\mathcal{T}_0$, such that

$$|T_{j_\ell+1}|/|T_{j_\ell}| \leq c_2 \qquad \text{and} \qquad |\hat{T}_{j_\ell}|/|\hat{T}_{j_\ell+1}| \leq c_2,$$

where $T_{j_\ell} \subseteq \hat{T}_{j_\ell} \in \mathcal{T}_0$ and $T_{j_\ell+1} \subseteq \hat{T}_{j_\ell+1} \in \mathcal{T}_0$. The definition of $\ell(T_j)$ gives the estimate

$$\ell(T_{j_\ell+1}) - \ell(T_{j_\ell}) = \log_2 \sqrt{|\hat{T}_{j_\ell+1}|/|T_{j_\ell+1}|\,|T_{j_\ell}|/|\hat{T}_{j_\ell}|} \leq \log_2 c_2.$$

In summary, we have

$$\ell(T_J) - \ell(T_1) \leq L \log_2 c_2 + \sum_{\ell=1}^{L-1} 3/2\,(j_{\ell+1} - j_\ell) \leq L \log_2 c_2 + \tfrac{3}{2} J.$$

This shows

$$\begin{aligned} |T|/d_z^2 = |T|2^{-3\delta(z,K)+2\ell(K)} &\leq |T|2^{-3J+3+2L\log_2 c_2+3J+2\ell(T_1)} \\ &= |T|8c_2^{2L}\,2^{2\ell(T_1)}. \end{aligned}$$

Recall that $z \in T \cap T_1$ and so the argument for the estimate for $\ell(T_{j_l+1}) - \ell(T_{j_l})$ applies and analogously shows

$$\ell(T_1) - \ell(T) \leq \log_2 c_2.$$

Then, for $T_1 \subseteq \hat{T}_1 \in \mathcal{T}_0$ and $T \subseteq \hat{T} \in \mathcal{T}_0$,

$$|T|/|\hat{T}|2^{2\ell(T_1)} = |T|/|\hat{T}|\ \ |\hat{T}_1|/|T_1| \leq c_2^2.$$

Hence, $|T|/d_z^2 \leq |\hat{T}|8c_2^{2(L+1)} =: c_1 - 1/|\hat{T}|$. ∎

Remark 4.1. From the proof it appears that c_1 in Proposition 4.1(b) depends on the mesh-size of the coarse grid. A different scaling of d_z, e.g., by multiplication with $\sqrt{|K_0|}$ for some fixed $K_0 \in \mathcal{T}_0$, results in a constant c_1 that depends on the ratio of different mesh-sizes in $\mathcal{T}_0$ only.

5. Proof of Theorem 1

The asserted H^1-stability in the theorem follows from the preceding Proposition 4.1 and Theorem 2 in [6]. To be self-contained and to verify the second inequality, we sketch the arguments and refer for more details to [6].

The mass matrix $M(T)$ of a triangle $T \in \mathcal{T}$ is a multiple of $M \in \mathbf{R}^{3\times 3}$ with $M_{jk} = 1 + \delta_{jk}$. Suppose $\lambda_1, \lambda_2, \lambda_3 > 0$ are the entries of the diagonal matrix Λ and satisfy $\lambda_1/\lambda_k \leq \sqrt{8} =: \kappa$. Then the eigenvalues of

$$\Lambda^{-1}A\Lambda \qquad \text{for} \quad A := (\Lambda^2 M + M\Lambda^2)/2$$

can be calculated as in [3]. Their smallest value is $5 - \mu$ for $\mu^2 := \sum_{j,k=1}^3 \lambda_j^2/\lambda_k^2 \leq 3 + 2(1 + \kappa^2 + \kappa^{-2}) = 21.25 < 25$. Hence A is positive definite and so $(x \cdot Ax)^{1/2}$ defines a norm for $x \in \mathbf{R}^3$. Consequently, we have

$$c_3^2 x \cdot \Lambda^2 M \Lambda^2 x \leq x \cdot Mx \leq c_4^2 x \cdot Ax = c_4^2 x \cdot \Lambda^2 Mx.$$

We will employ these estimates for $(\lambda_1, \lambda_2, \lambda_3) = h_T(1/d_a, 1/d_b, 1/d_c)$ for the three nodes a, b, c of T and d_z from Definition 4.1. The condition $\lambda_j/\lambda_k \leq \sqrt{8}$ follows from Proposition 4.1(a). Part (b) of which implies that c_3 and c_4 depend on c_1 but not on h_T.

Let P be a weak interpolation operator with $Pu \in \mathcal{S}_D^1(\mathcal{T})$ [5], [8], [7], [4] which satisfies

$$\|h_{\mathcal{T}}^{-1}(u - Pu)\|_{L^2(\Omega)} + \|\nabla Pu\|_{L^2(\Omega)} \leq c_5\|\nabla u\|_{L^2(\Omega)}$$

with the local mesh-size $h_{\mathcal{T}} \in L^\infty(\Omega)$, $h_{\mathcal{T}}|_T = h_T$ on $T \in \mathcal{T}$. The constant c_5 depends on the shape of the triangles and so on $\mathcal{T}_0$ only. Then, let $q_h := Pu - \Pi u = \sum_{\ell=1}^n q_\ell \varphi_\ell \in \mathcal{S}_D^1(\mathcal{T})$ for the nodal basis $(\varphi_1, \ldots, \varphi_n)$ of $\mathcal{S}_D^1(\mathcal{T})$ and let $p_h := \sum_{\ell=1}^n q_\ell d_\ell^{-2}\varphi_\ell \in \mathcal{S}_D^1(\mathcal{T})$ so that

$$q_h|_T = \sum_{\ell=1}^n q_\ell \varphi_\ell|_T = \sum_{j=1}^3 \xi_{T,j}\psi_{T,j} \quad \text{on} \quad T \in \mathcal{T}_0$$

for coefficient vectors $x_T = (\xi_{T,1}, \xi_{T,2}, \xi_{T,3}) = (q_{\ell(T,1)}, q_{\ell(T,2)}, q_{\ell(T,3)})$. An elementwise inverse estimate gives $\|\nabla q_h\|_{L^2(\Omega)} \leq c_6\|h_{\mathcal{T}}^{-1}q_h\|_{L^2(\Omega)}$. A triangle inequality shows

$$\begin{aligned}\|\nabla \Pi u\|_{L^2(\Omega)} &\leq \|\nabla Pu\|_{L^2(\Omega)} + \|\nabla q_h\|_{L^2(\Omega)} \\ &\leq c_5\|\nabla u\|_{L^2(\Omega)} + c_6\|h_{\mathcal{T}}^{-1}q_h\|_{L^2(\Omega)}\end{aligned}$$

and it remains to bound $\|h_{\mathcal{T}}^{-1} q_h\|_{L^2(\Omega)}$. With the mass matrix $M(T)$ of T, this reads

$$
\begin{aligned}
\|h_{\mathcal{T}}^{-1} q_h\|_{L^2(\Omega)}^2 &= \sum_{T\in\mathcal{T}} h_T^{-2}\, x_T \cdot M(T) x_T \\
&\le c_4^2 \sum_{T\in\mathcal{T}} h_T^{-2}\, x_T \cdot \Lambda(T)^2 M(T) x_T \\
&= c_4^2 \sum_{T\in\mathcal{T}} \sum_{j=1}^{3} \frac{q_{\ell(T,j)}}{d_{\ell(T,j)}^2} \int_T \varphi_{\ell(T,j)} q_h \, dx \\
&= c_4^2 \int_\Omega p_h q_h \, dx,
\end{aligned} \tag{1}
$$

where we used the above estimate and $d_{\ell(T,j)} = d_z$ for the node z with hat function $\varphi_{\ell(T,j)}$ with global number $\ell(T, j)$ and local number j in T. Since Π is the L^2 projection,

$$
\int_\Omega p_h q_h \, dx = \int_\Omega p_h (p_h - u)\, dx \le c_5 \|h_{\mathcal{T}} p_h\|_{L^2(\Omega)} \|\nabla u\|_{L^2(\Omega)}.
$$

The above estimates then yield (since $\Lambda^2 x_T$ are the nodal values of p_h)

$$
\|h_{\mathcal{T}} p_h\|_{L^2(\Omega)}^2 = \sum_{T\in\mathcal{T}} h_T^2 x_T \cdot \Lambda^2 M \Lambda^2 x_T \le 1/c_3^2 \, \|h_{\mathcal{T}}^{-1} q_h\|_{L^2(\Omega)}^2. \tag{2}
$$

The combination of the last three inequalities concludes the proof of the first estimate on the H^1-norms.

The proof of the second uses the aforementioned arguments for $q_h := Pu$ and $p_h := \sum_{\ell=1}^n q_\ell d_\ell^{-2} \varphi_\ell \in \mathcal{S}_D^1(\mathcal{T})$. Formulas (1) and (2) remain valid and are combined with $\int_\Omega p_h q_h \, dx = \int_\Omega p_h u \, dx$. This shows

$$
\|h_{\mathcal{T}}^{-1} \Pi u\|_{L^2(\Omega)} \le c_4^2/c_3 \|h_{\mathcal{T}}^{-1} u\|_{L^2(\Omega)}. \qquad \blacksquare
$$

Remark 5.1. Proposition 4.1 holds for a class of triangulations into parallelograms and triangles as well, but the mass matrices $M(T)$ do not allow a positive definite matrix $\Lambda^{-1} A \Lambda$ if T is a parallelogram.

Remark 5.2. The author expects similar results for three-dimensional domains. Details, however, are less obvious.

Acknowledgments. This paper was completed during a visit to the Newton Institute, Cambridge, England.

References

1. D. N. ARNOLD, A. MUKHERJEE, L. POULY (2000): *Locally adapted tetrahedral meshes using bisection*. SIAM J. Sci. Comput., **22**(2):431–448 (electronic).
2. E. BÄNSCH (1991): *Local mesh refinement in* 2 *and* 3 *dimensions*. IMPACT Comput. Sci. Engng., **3**:181–191.

3. J. H. BRAMBLE, J. E. PASCIAK, O STEINBACH (2001): *On the stability of the L_2-projection in $H^1(\Omega)$*. Math. Comp., **71**(237):147–156.
4. S. C. BRENNER, L. R. SCOTT (1994): The Mathematical Theory of Finite Element Methods, Texts in Applied Mathematics, Vol. 15. New York: Springer-Verlag.
5. C. CARSTENSEN (1999): *Quasi-interpolation and a posteriori error analysis in finite element method*. M2AN, **33**:1187–1202.
6. C. CARSTENSEN (2001): *Merging the Bramble–Pasciak–Steinbach and the Crouzeix–Thomée criterion for H^1-stability of the L^2-projection onto finite element spaces*. Math. Comp., **71**(237):157–163.
7. P. G. CIARLET (1978): The Finite Element Method for Elliptic Problems. Amsterdam: North-Holland.
8. P. CLÉMENT (1975): *Approximation by finite element functions using local regularization*. RAIRO Sér. Rouge Anal. Numér., **R-2**:77–84.
9. M. CROUZEIX, V. THOMÉE (1987): *The stability in L^p and $W^{1,p}$ of the L^2-projection onto finite element function spaces*. Math. Comp., **48**:521–532.
10. J. M. MAUBACH (1995): *Local bisection refinement for n-simplicial grids generated by reflection*. SIAM J. Sci. Comput., **16**(1):210–227.
11. W. F. MITCHELL (1989): *A comparison of adaptive refinement techniques for elliptic problems*. ACM Trans. Math. Software, **15**(4):326–347.
12. M. C. RIVARA (1984): *Algorithms for refining triangular grids suitable for adaptive and multigrid techniques*. Internat. J. Numer. Methods Engng., **20**:745–756.
13. O. STEINBACH (2002): *On the stability of the L_2-projection in fractional Sobolev spaces*. Numer. Math., **90**(4):775–786.
14. R. VERFÜRTH (1996): A Review of a Posteriori Error Estimation and Adaptive Mesh-Refinement Techniques. New York: Wiley-Teubner.

C. Carstensen
Institute for Applied Mathematics and Numerical Analysis
Vienna University of Technology
Wiedner Hauptstrasse 8-10
A-1040 Vienna
Austria
carsten.carstensen@tuwien.ac.at